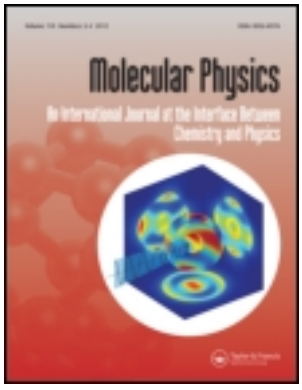

Molecular Physics: An International Journal at the Interface Between Chemistry and Physics
Publication details, including instructions for authors and subscription information:
http://www.tandfonline.com/loi/tmph20

The mechanism of the amine-catalysed isomerization of dialkyl maleate: a computational study

Rafik Karaman [a] , Sabino A. Bufo [b] , Laura Scrano [b] & Hussein Hallak [a]

[a] Department of Bioorganic Chemistry, Faculty of Pharmacy,Al-Quds University, P.O. Box 20002, Jerusalem

[b] Department of Agriculture, Forestry and Environment, University of Basilicata, Via dell'Ateneo Lucano 10, 85100, Potenza, Italy

Accepted author version posted online: 10 Jan 2012.Version of record first published: 01 Feb 2012.

To cite this article: Rafik Karaman, Sabino A. Bufo, Laura Scrano & Hussein Hallak (2012): The mechanism of the amine-catalysed isomerization of dialkyl maleate: a computational study, Molecular Physics: An International Journal at the Interface Between Chemistry and Physics, 110:8, 467-482

To link to this article: http://dx.doi.org/10.1080/00268976.2012.655794

Molecular Physics
Vol. 110, No. 8, 20 April 2012, 467–482

Taylor & Francis
Taylor & Francis Group

RESEARCH ARTICLE

The mechanism of the amine-catalysed isomerization of dialkyl maleate: a computational study

Rafik Karaman[a]*, Sabino A. Bufo[b], Laura Scrano[b] and Hussein Hallak[a]

[a]*Department of Bioorganic Chemistry, Faculty of Pharmacy,Al-Quds University, P.O. Box 20002, Jerusalem;*
[b]*Department of Agriculture, Forestry and Environment, University of Basilicata, Via dell'Ateneo Lucano 10, 85100, Potenza, Italy*

(*Received 17 October 2011; final version received 23 December 2011*)

DFT at B3LYP/6-31G (d,p) level calculation results for the amine-catalysed isomerization of dimethyl maleate revealed that the mechanism proceeds via four steps: (1) a concerted proton transfer from one amine molecule to another which subsequently enhances the addition of the adduct thus formed to the C–C double bond to yield INT1. (2) Abstraction of a proton from the β-carbon of INT1 by a second amine molecule to give intermediate INT2. (3) Rotation about the C–C single bond followed by proton abstraction by an amine molecule to yield unstable INT3, and (4) an elimination of an amine molecule to yield the trans isomer, dimethyl fumarate. Furthermore, it was found that step 1 is the rate limiting step. However, the activation energy difference between steps 1 and 2 was significantly low and its value depends on the amine catalyst used. The activation energy was found to be lower in water when compared to that calculated in the gas phase. In addition, linear correlation was found between the amine-catalysed isomerization experimental rate and the p*K*a of the amine catalyst on one hand and the enthalpic and free activation energies on the other hand. The calculations also confirmed that the reaction is first order in dimethyl maleate, second order in the amine catalyst and overall third order. This study disproves three of the four different intermediates that were previously suggested to explain the amine catalysed isomerization of dialkyl maleates. The study verifies the intermediate suggested by Rappoport.

Keywords: dimethyl maleate; isomerization of dimethyl maleate; dimethyl fumarate; DFT calculations; amine-catalysed *cis-trans* isomerization

1. Introduction

While maleic acid, in which the alkene double bond is in conjugation with a carboxyl group, is a synthetic organic compound, its *trans* isomer, fumaric acid, and is an organic acid found in plants, in humans and in other mammals. It is a key intermediate in the citric acid cycle. Maleic acid is highly useful as an intermediate in the industrial preparations of polyester resins, plasticizers, copolymers, and agricultural chemicals. Fumaric acid is used by cells to produce energy from food. Human skin naturally produces fumaric acid when exposed to sunlight. It is used as a food acidulant and also as an intermediate in the synthesis of certain polyester resins, furniture lacquers, paper sizing chemicals and aspartic acid [1].

Maleic acid and fumaric acid cannot normally interconvert because rotation around the carbon-carbon double bond is restricted. In the laboratory, maleic acid and its corresponding methyl ester, dimethyl maleate, undergo isomerization on treatment with catalytic amounts of aqueous bromine or under UV light to form the thermodynamically more stable *trans* isomer. On treatment with slight excess of bromine the reaction gives the addition product selectively when heated to 77°C. Treatment of dimethyl maleate with excess bromoform under UV irradiation for few days gives selectively the isomerized product in 95% yield *via* bromine that released as an intermediate. The bromine-catalysed reaction is attributed to the reversible addition of a bromine radical at the site of the double bond [2]. Further, it was reported that the NBS-bromination condition is sufficient for (Z)-to (E)-alkene isomerization. Dimethyl maleate on treatment with NBS-AIBN (N-bromosuccinimide dibenzoyl peroxide-azobisisobutyronitrile) reagent gives dimethyl fumarate in very high yield. Isomerization of the carbon–carbon double bond takes place via an *in situ* addition–elimination of the bromine radical [3].

The electrochemical reduction of dimethyl maleate and dimethyl fumarate in acetonitrile and methanol solutions has been investigated using cyclic voltammetry, rotating ring-disk electrode voltammetry and in situ FT-IR spectroelectrochemistry. In both solvents,

*Corresponding author. Email: dr_karaman@yahoo.com

ISSN 0026–8976 print/ISSN 1362–3028 online

http://dx.doi.org/10.1080/00268976.2012.655794
http://www.tandfonline.com

the electrochemically generated radical anion of dimethyl maleate undergoes both a rapid *cis–trans* isomerization process forming the dimethyl fumarate radical anion and a rapid radical anion dimerization reaction [4].

Cis-trans isomerization catalysed by amines has been known for almost a century. *Cis–trans* isomerization catalysed by nucleophiles has been documented in the case of dialkyl maleate and fumarate. It has been shown that ammonia, primary amines and secondary amines readily catalyse the isomerization of dialkyl maleate to the corresponding fumarate esters. For instance, a trace of piperidine transforms methylmaleate in a few seconds into a crystalline mass of the fumarate, and since the former has much greater energy content, the temperature rises considerably. Dimethylamine, diethylamine, piperazine, methylamine, allylamine, benzylamine, *d*- and *l*- phenylethylamine, β-phenylethylamine, coniine, and aniline also effect the change, although some of them do not bring about a complete transformation. Tertiary amines such as triethylamine, dimethylaniline, diethylaniline, and pyridine, however, do not catalyse the inversion, although triethylamine is a much stronger base than many of the above primary and secondary ones [5–8]. Enamines cause the maleate to fumarate isomerization to take place through zwitterions intermediate. These esters can also add reversibly across the carbon–carbon double bond of the enamine to give a cyclobutane derivative, or they can add irreversibly to the enamine's carbon to give substituted succinate esters. The amine moiety of aminals adds to dimethyl maleate *via* azomethine yield intermediates to furnish dimethyl fumarate. For example, at room temperature the pyrrolidine aminal of isobutyraldehyde catalyses the isomerization of dimethyl maleate to dimethyl fumarate [9].

Cis –trans isomerization of dimethyl maleate to fumarate by the addition of protic imidazolium species was also reported. The feasibility of a quantitative *cis–trans* isomerization of dimethyl maleate to fumarate was established. The suggested mechanism relies on the addition of protic imidazolium species to carbon–carbon double bond, followed by rotation and final imidazolium elimination [10].

In earlier studies, a mechanism was proposed for the acid and salt catalysed isomerization of maleic acid to fumaric acid. The mechanism assumed the formation of an intermediate which involved both a proton donor and an electron donor (anion). Since amines could serve both as proton and electron donors it has been assumed that the *cis-trans* amine-catalysed isomerization is due to the formation of an intermediate [6–8].

The mechanism proposed by Nozaki for the amine-catalysed isomerization is similar to that proposed for the isomerization catalysed by inorganic acids and salts [6]. As in the other mechanism Nozaki's intermediate (intermediate 1, Figure 1) is assumed to have the same probability of decomposing into the maleate or the fumarate due to the equivalence of the two bonds between C1 and C2 in the complex. The completeness of isomerization is explained by a difference in the energy of activation of the rate determining step for the maleate and the fumarate. The reaction was assumed to involve preliminary association between a molecule of amine and ester before reaction with another molecule of amine. The mechanism predicts that the isomerization reaction should be of first order with respect to ester and of second order with respect to amine. Since a proton is necessary for association with the carbonyl oxygen, tertiary amines would not be expected to have any catalytic effect. According to the mechanism stronger bases, because of their ability to readily donate a pair of electrons, might be expected to be better catalysts for isomerization. Later on, the mechanism proposed by Nozaki was corrected by Davies and Evans [7] who, however, preferred intermediate 2 (Figure 1) by which two molecules of amine coordinate with the two carbonyl oxygens of the ester moiety. Intermediate 3, (Figure 1) tentatively suggested by Eliel [11] as a product of 1,4-addition, explains neither the third-order kinetics nor the unreactivity of tertiary amines in the reaction, unless the mechanism is a concerted one, as otherwise a planar carbanion, capable of isomerization should be formed in the first, nucleophilic, addition step of this mechanism. The formation of intermediate 4 (Figure 1) suggested by Rappoport [8] was explained on the basis that in the maleate system, with the attacked carbon atom activated only by one alkylcarbonyl group, and with even this effect diminished by the symmetry of the molecule, direct nucleophilic attack by amines is difficult. The attack can be easier when a four-centre α,β-addition can take place, as with primary and secondary amines. Formation of a planar carbanion is not required in the first step of this mechanism and stereoselective elimination of the amine from intermediate 4 gives the fumarate. However, the tertiary amino-group in intermediate 4 bound to a carbon atom bearing an electron-withdrawing group, cannot compete seriously for the proton with free amine molecules, the necessary presence of which in the rate-determining step gives the overall third-order kinetics [8].

Another interest in the amine-catalysed isomerization of dialkylmaleate comes from the biochemistry field. Maleylacetoacetate isomerase

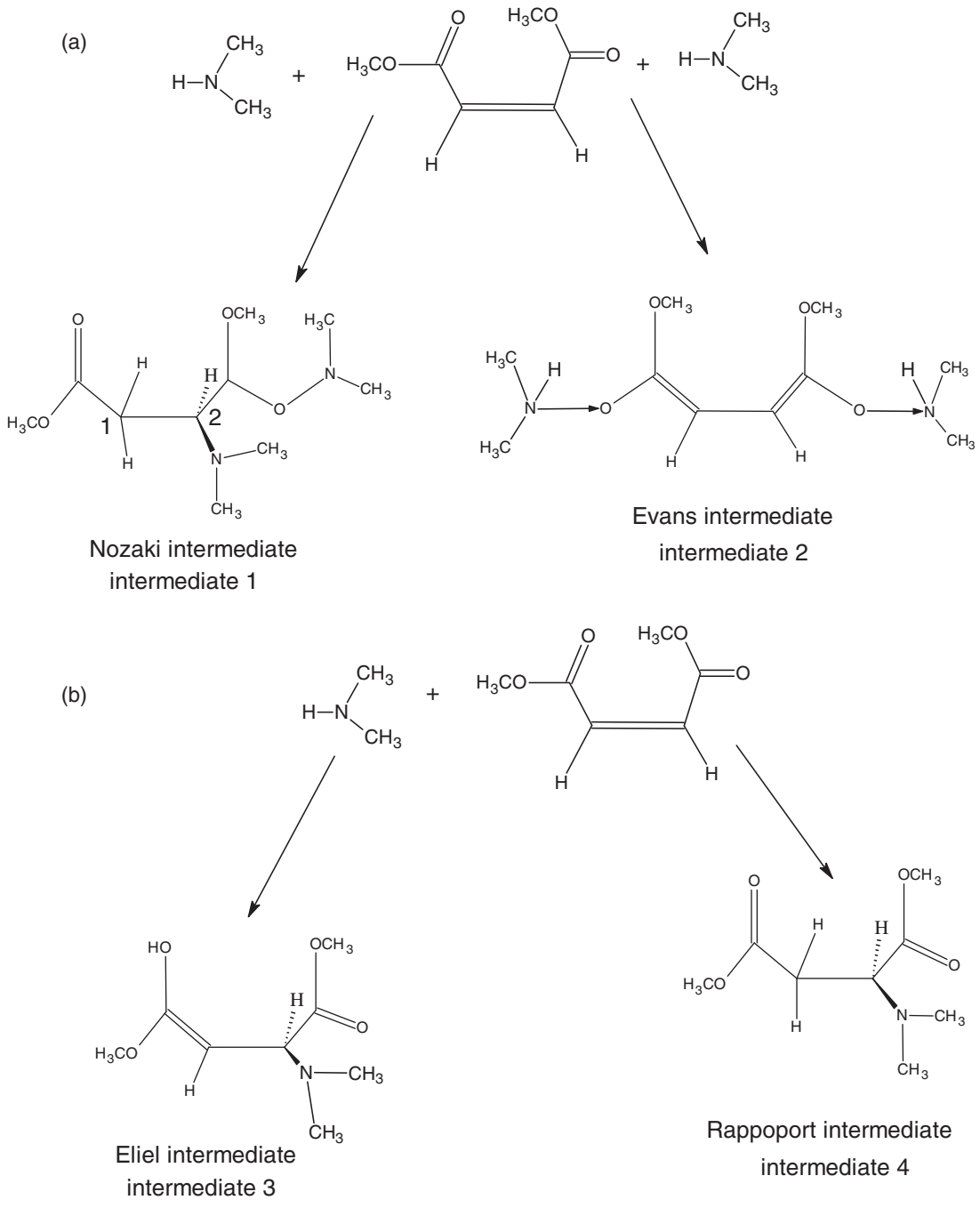

Figure 1. (a) Proposed intermediates for the isomerization of dimethyl maleate to dimethyl fumarate in the presence of 2 equivalent of amine. (b) Proposed intermediates for the isomerization of dimethyl maleate to dimethyl fumarate in the presence of 1 equivalent of an amine.

(MAAI), a key enzyme in the metabolic degradation of phenylalanine and tyrosine, catalyses the glutathione-dependent isomerization of maleylacetoacetate to fumarylacetoacetate (eq. 1). Deficiencies in enzymes along the degradation pathway lead to serious diseases including phenylketonuria, alkaptonuria, and the fatal disease, hereditary tyrosinemia type I [12–14].

$$4-\text{maleylacetoacetate} \overset{\text{MMAI}}{\rightleftharpoons} 4-\text{fumarylactoacetate} \quad (1)$$

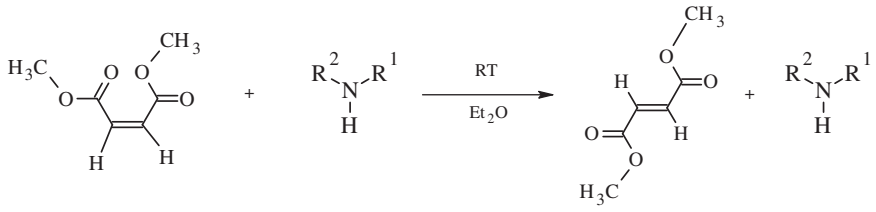

1 $R^1 = R^2$ = Methyl
2 R^1 = H; R^2 = Methyl
3 R^1 = H; R^2 = Ethyl
4 R^1 = H; R^2 = Phenyl
5 R^1 = H; R^2 = Benzyl
6 Amine = Piperidine
7 R^1 = H; R^2 = Hydroxyethyl
8 R^1 = H; R^2 = Aminoethyl

Scheme 1. Amine-catalysed isomerization of **1**–**8**.

Recent studies reveal that dimethyl fumarate can be used to treat psoriasis, but there are risk factors involved upon ingestion of this compound. Reactivity of dimethyl fumarate towards glutathione in the preparation of S-substituted thiosuccinic acid esters and its presystemic metabolism has been reported. It has been also reported that fumaric acid could be a cure for the inflammatory disease multiple sclerosis (MS). Fumaric acid, however, is not an ideal treatment for a chronic disease. It causes flushing and some unpleasant gastrointestinal side effects. Recently, researches began developing fumaric acid derivatives that maximized efficacy while minimizing side effects. One of these was dimethyl fumarate, however its bioavailability was low due to fast degradation upon exposure to physiological environment [15–18].

The main goal of this work was to investigate the mechanism and the factors affecting the reaction rate of the amine-catalysed isomerization of dimethyl maleate to dimethyl fumarate. Unraveling the mechanism of the amine-catalysed isomerization will shed light on the kinetics and thermodynamics of the *cis-trans* conversion when using various types of amines having different p*K*a as a catalyst. The results of this study will be exploited in designing prodrugs that will have the potential to have higher bioavailability than their parental drugs [19–23].

Since a variety of different intermediates were suggested to explain the *cis-trans* isomerization of dialkyl maleates the computational efforts were directed toward the elucidation of the transition states, intermediates and ground state structures for all possible pathways in the isomerization of **1**–**8** (Scheme 1).

2. Methods

The Becke three-parameter, hybrid functional [24] combined with the Lee, Yang, and Parr correlation functional [25], denoted B3LYP [26], were employed in the calculations using density functional theory (DFT). All calculations were carried out using the quantum chemical package Gaussian-2009 [27]. Calculations were carried out based on the restricted Hartree–Fock method [27]. The starting geometries of all calculated molecules **1**–**8** were obtained using the Argus Lab program [28] and were initially optimized at the HF/6-31G level of theory followed by optimization at the B3LYP/6-31G(d,p). Second derivatives were estimated for all 3N-6 geometrical parameters during optimization. An energy minimum (a stable compound or a reactive intermediate) has no negative vibrational force constant. A transition state is a saddle point which has only one negative vibrational force constant [29]. Transition states were located first by the normal reaction coordinate method [30] where the enthalpy changes was monitored by stepwise changing the interatomic distance between two specific atoms. The geometry at the highest point on the energy profile was re-optimized by using the energy gradient method at the B3LYP/6-31G(d,p) level of theory [27]. The 'reaction coordinate method' [30] was used to calculate the activation energy in **1**–**8** (Schemes 1). In this

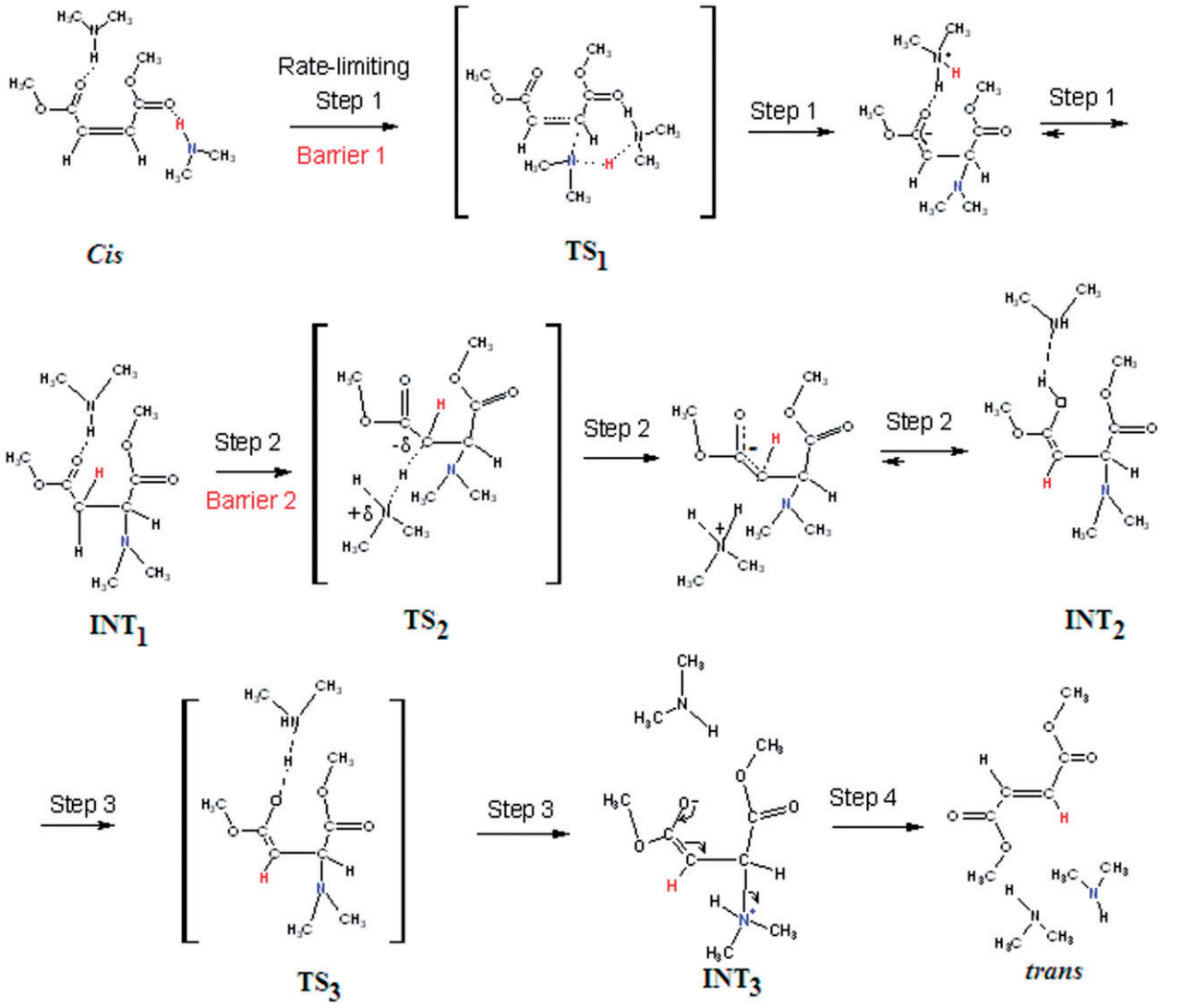

Scheme 2. Mechanistic pathway for the amine-catalysed isomerization of dimethyl maleate into dimethyl fumarate. Dimethylamine was chosen to represent the various amines apart from tertiary amines.

method, one bond length is constrained for the appropriate degree of freedom while all other variables are freely optimized. The activation energy values for the first step in the process (the approach of the amine nitrogen towards the carbon of the C–C double bond, Scheme 3) were calculated from the difference in energies of the global minimum structures (GM) and the derived transition states (TS_1 in Scheme 2). Similarly, the activation energies for step 2 (an abstraction of a proton from INT1 by an amine molecule) were calculated from the difference in energies of the global minimum structures (GM) and the corresponding transition states (TS_2 in Scheme 2). Verification of the desired reactants and products was accomplished using the 'intrinsic coordinate method' [30]. The transition state structures were verified by their only one negative frequency. Full optimization of the transition states was accomplished after removing any constrains imposed while executing the energy profile. The activation energies obtained from the DFT at B3LYP/6-31G (d,p) level of theory for **1**–**8** were calculated with and without the inclusion of solvent (water and ether). The calculations with the incorporation of a solvent were performed using the integral equation formalism model of the Polarizable Continuum Model (PCM) [31–34]. In this model the cavity is created via a series of overlapping spheres. The radii type employed was the United Atom Topological Model on radii optimized for the PBE0/6-31G (d) level of theory.

3. Results and discussion

3.1. *Calculations of thermodynamic stability for intermediates 1–4*

Using the package Gaussian 2009 [24] the DFT B3LYP/6-31G (d,p) structures and energies for the previously proposed four intermediates 1–4 (Figure 1) were calculated. In order to estimate the relative stabilities of intermediates 1–4 the corresponding global minimum structures were calculated as well (Figure 1). The DFT optimized geometries of Nozaki's and Evans's intermediates (intermediates 1 and 2 in Figure 1) revealed that both structures are entirely unstable and undergo dissociation back to the corresponding reactants. This was observed upon full optimization of the intermediates after removing any constrains imposed while executing the optimization of the fixed geometries suggested by Nozaki and Evans. In addition, The DFT results demonstrated that Rappoport's [8] intermediate 4 was the most stable among the four proposed intermediates where its free energy was about 5.77 kcal/mol less than the energy of its reactants. On the other hand, the difference in energy between Elil's [11] intermediate 3 and the corresponding reactant was 24.24 kcal/mol.

3.1.1. *Calculations of activation energy for the reaction leading to Rappoport intermediates 4*

Since Rappoport's intermediate 4 was found to be the most stable among the proposed four intermediates attempts were made to locate the transition state leading to it. Scheme 3 illustrates the pathway by which one molecule of amine approaches one of the C–C double bond carbons. The DFT calculations for the structures shown in Scheme 3 revealed that although the activation energy for the reaction of dimethyl maleate with one molecule of dimethylamine to yield Rappoport's intermediate 4 is relatively low the direction of the reaction is towards the reactants. This was revealed upon full optimization of Rappoport's intermediate structure that resulted in dissociation back to the reactants (global minimum structure). Imposing constrains on the geometry of intermediate 4 resulted in a conformation having high energy. This is due to the fact that in the maleate system with the attacked carbon atom activated only by one methoxy carbonyl group direct nucleophilic attack by amines is difficult. The attack will be easier when a four-centre α,β-addition can take place. However, the tertiary amino-group in intermediate 4, bound to a carbon atom bearing an electron-withdrawing group, cannot compete seriously for the proton with free amine molecules,

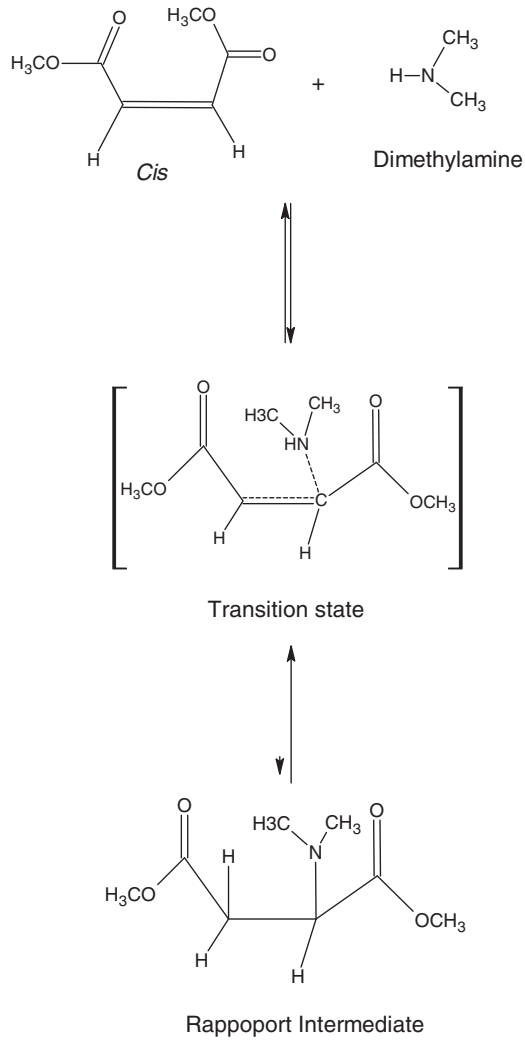

Scheme 3. Isomerization of dimethyl maleate in the presence of one molecule of amine as a catalyst via the formation of Rappoport's intermediate 4.

the necessary presence of which in the rate-determining step gives the overall third-order kinetics. This conclusion is in accordance with previous observation by Rappoport [8].

It can be concluded from the above mentioned results that the amine-catalysed isomerization should proceed by a mechanism by which two molecules of amine are involved in the reaction rate-limiting step.

Scheme 2 shows the amine-catalysed isomerization of dimethyl maleate by which two molecules of an amine are participating in the rate-limiting step. The enthalpic and entropic energies in the gas phase for the global minimum structure (*cis*), the three different transition states, TS_1, TS_2 and TS_3, the three different

Table 1. DFT (B3LYP/6-31G (d,p)) calculated properties for the amine-catalysed isomerization in **1**–**8**.

Comp.	Enthalpy, H (gas phase) In hartree	Entropy Cal/mol-kelvin	Frequency cm^{-1}	Comp.	Enthalpy, H (gas phase) In hartree	Entropy Cal/mol-kelvin	Frequency cm^{-1}
1*Cis*	−804.71206	167.78	–	**5*Cis***	−1188.211242	205.75	–
1TS$_1$	−804.69105	145.03	1045.16i	**5TS$_1$**	−1188.186306	180.53	1044.79i
1INT$_1$	−804.72753	163.37	–	**5INT$_1$**	−1188.231211	195.76	–
1TS$_2$	−804.69059	157.04	1180.67i	**5TS$_2$**	−1188.190533	194.75	1181.58i
1INT$_2$	−804.69786	155.63		**5INT$_2$**	−1188.201668	195.91	
1*Trans*	−804.71816	183.82	–	**5*Trans***	−1188.219047	213.57	–
2*Cis*	−726.09148	163.13	–	**6*Cis***	−1038.202341	158.02	–
2TS$_1$	−726.07438	134.58	1013.97i	**6TS$_1$**	−1038.178047	162.53	1108.86i
2INT$_1$	−726.11106	149.83	–	**6INT$_1$**	−1038.225612	182.47	–
2TS$_2$	−726.07207	141.13	1155.75i	**6TS$_2$**	−1038.181468	178.48	1215.75i
2INT$_2$	−726.08202	146.55		**6INT$_2$**	−1038.187232	165.78	
2*Trans*	−726.09923	165.44	–	**6*Trans***	−1038.213605	191.00	–
3*Cis*	−804.73155	176.56	–	**7*Cis***	−955.144823	187.88	–
3TS$_1$	−804.71308	147.62	1029.15i	**7TS$_1$**	−955.121171	156.92	1049.06i
3INT$_1$	−804.75092	164.04	–	**7INT$_1$**	−955.165212	177.92	–
3TS$_2$	−804.71160	154.59	1174.95i	**7TS$_2$**	−955.122459	168.86	1159.10i
3INT$_2$	−804.72230	158.07		**7INT$_2$**	−955.135561	172.94	
3*Trans*	−804.73869	179.13	–	**7*Trans***	−955.153108	193.49	–
4*Cis*	−1109.59990	187.18	–	**8*Cis***	−915.419221	190.70	–
4TS$_1$	−1109.56148	166.71	1105.03i	**8TS$_1$**	−915.400902	163.57	1035.10i
4INT$_1$	−1109.61693	179.20	–	**8INT$_1$**	−915.440038	175.85	–
4TS$_2$	−1109.56508	168.05	1174.12i	**8TS$_2$**	−915.399322	169.24	1170.00i
4INT$_2$	−1109.57624	170.78		**8INT$_2$**	−915.409753	166.91	
4*Trans*	−1109.60680	178.67	–	**8*Trans***	−915.428024	193.35	–

Note: Cis, INT, TS and Trans are optimized reactant, intermediate, transition state and product structures, respectively (see Scheme 2).

intermediates INT_1, INT_2 and INT_3 and the product (*trans*) for the pathways in **1**–**8** were calculated. Table 1 summarizes the energy values for **1*Cis*-8*Cis***, **1TS$_1$-8TS$_1$**, **1INT$_1$-8INT$_1$**, **1TS$_2$-8TS$_2$**, **1INT$_2$-8INT$_2$** and **1*Trans*-8*Trans***. Figure 2a–f illustrate the gas phase DFT optimized calculated structures for *Cis*, TS_1, INT_1, TS_2, INT_2 and *Trans* in **1**–**8**.

3.2. *Conformational analysis for the chemical entities involved in the amine-catalysed isomerization of 1–8*

3.2.1. *Starting geometries (*Cis *isomers)*

Figure 2(a) illustrates the DFT optimized structures for the reactants in **1**–**8** and Table 1 lists their calculated energies. Inspection of Figure 2(a) indicates that the dimethyl maleate moiety was found to reside in asymmetrical geometry by which the two carbonyl groups are positioned in a vertical orientation one to the other. In addition, it indicates that the global minimum structures for the reactants exhibit conformations by which the two amine molecules hydrogen bond with the dimethyl maleate carbonyl groups. The length of the hydrogen bond varies according to the nature of the amine. The hydrogen bond length was found in the range 2.09–2.32 Å. The C–C double bond in all the systems was identical with a length of 1.34 Å. The values of the two C–C double bond angles were different. While for one of them the range was 124.0°–124.6° for the other it was 126.3°–127.1°.

3.2.2. *Transition state TS_1*

The calculated DFT optimized structures for the first transition states (TS_1) in the isomerization of **1**–**8** are summarized in Table 1 and are shown in Figure 2(b). As shown in Figure 2(b) the transition state was achieved when one molecule of an amine was approaching one of the C–C double bond carbons and at the same time another amine molecule was approaching the amine hydrogen of the quaternary ammonium thus formed (Scheme 2). The breaking and forming bonds in all transition states were similar. The distance N—H was 1.315 Å and the angle N/H/N was 155°. The C-N distance length for **1TS1-8TS1** was in the range 1.53–1.56 Å and the C–C bond α to the carbonyl was identical in all transition states with a value of 1.48 Å. It should be emphasized that an existence of a hydrogen bond between the amine hydrogen and one of the carbonyls contributes much to the stabilization of **1TS1-8TS1**. The hydrogen bond

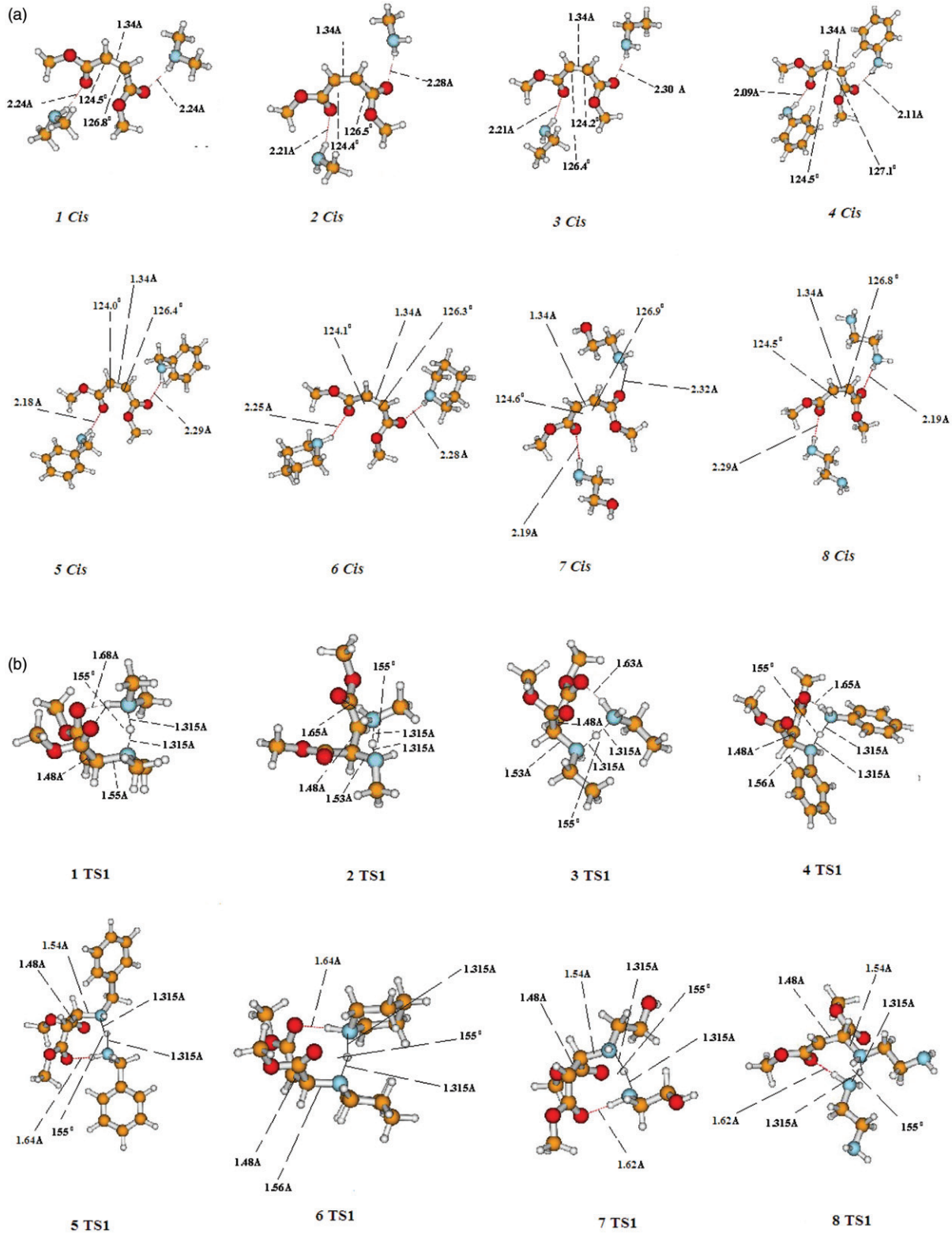

Figure 2. (a) B3LYP/6-31G (d,p) optimized structures for the reactants (**1Cis-8Cis**) in processes **1–8**. (b) B3LYP/6-31G (d,p) optimized structures for the transition states **1TS1-8TS1** in processes **1–8**. (c) B3LYP/6-31G (d,p) optimized structures for intermediates **1NT1-8INT1** in processes **1–8**. (d) B3LYP/6-31G (d,p) optimized structures for intermediates **1TS2-8TS2** in processes **1–8**. (e) B3LYP/6-31G (d,p) optimized structures for intermediates **1INT2-8INT2** in processes **1–8** (f) B3LYP/6-31G (d,p) optimized structures for intermediates **1Trans-8Trans** in processes **1–8**.

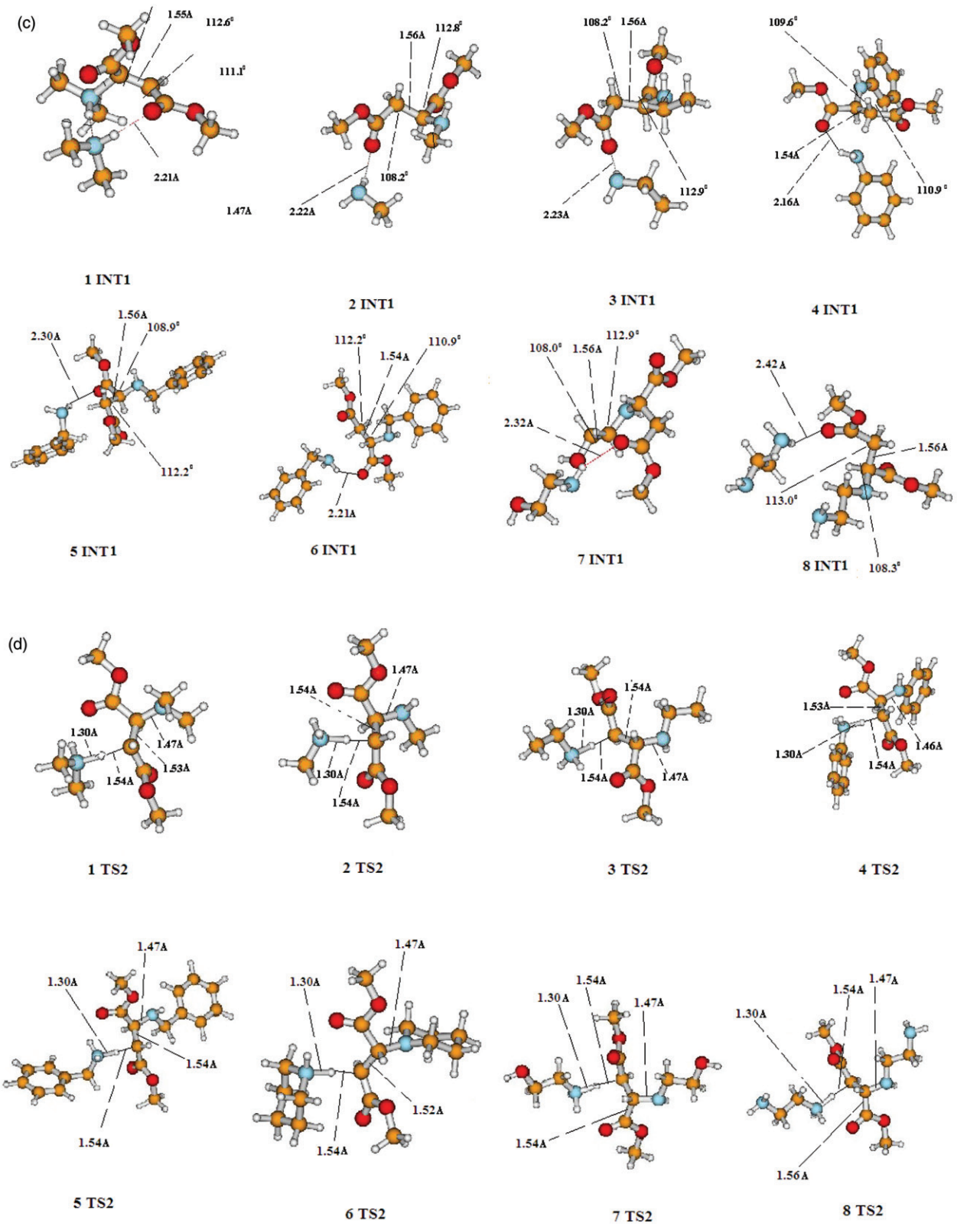

Figure 2. Continued.

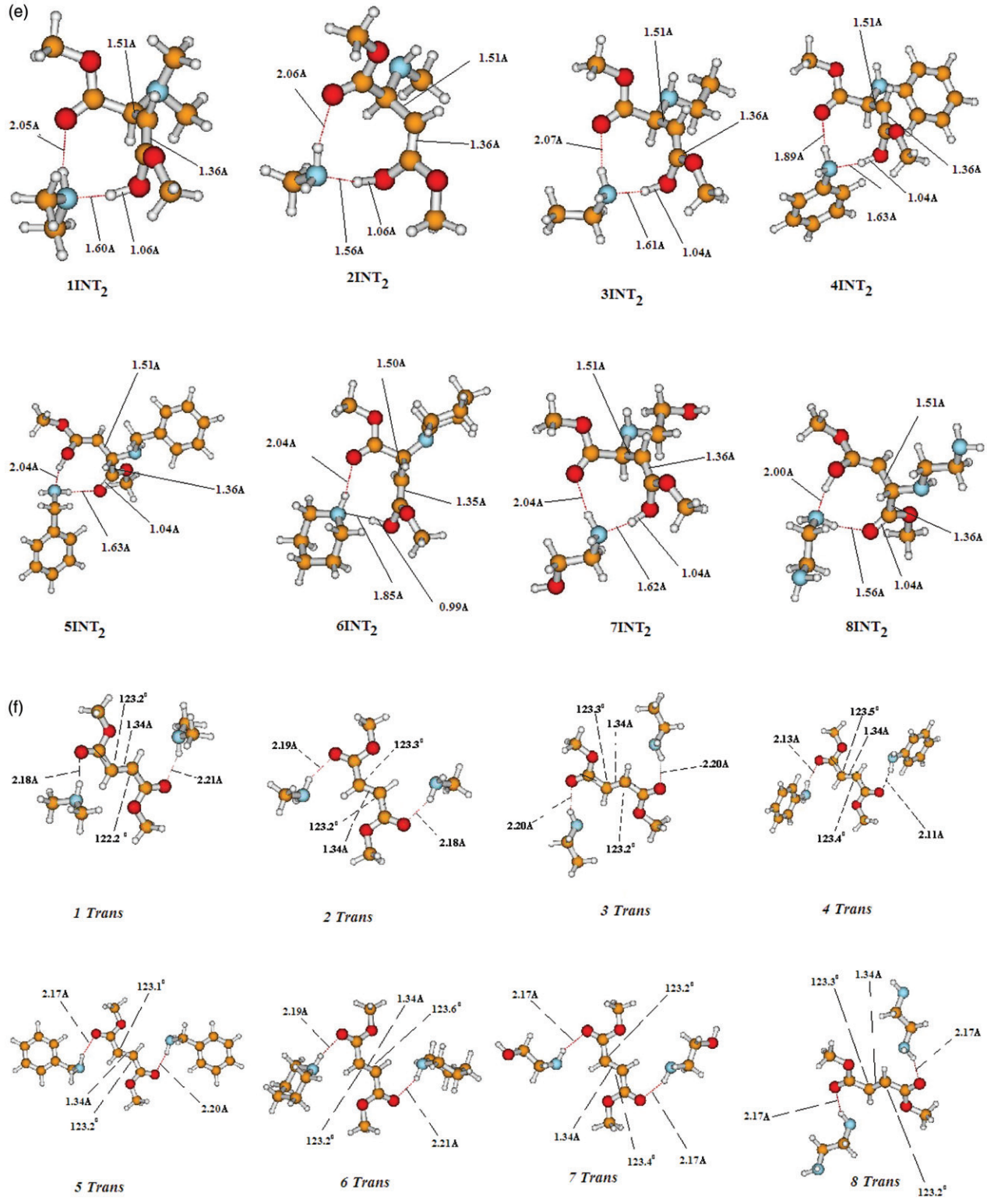

Figure 2. Continued.

NH—(O)C in **1TS-8TS** was found in the range 1.62–1.64 Å.

3.2.3. *Intermediate INT$_1$*

The calculated DFT geometries for the tetrahedral intermediates in **1–8** (**1NT1-8INT1**) are shown in Figure 2(c) and their parameters are listed in Table 1. Careful inspection of the values in Figure 2(c) revealed that the C–C bond angles α to the carbonyl are reduced when compared with that in the corresponding reactants. These values were found in the range 108°–113° similar to that for regular tetrahedral intermediates. The length of the C–C bond α to the carbonyl was similar in all intermediates with a value of 1.54–1.56 Å. The free amine molecule was found to hydrogen bond with one of the intermediate carbonyls. The hydrogen bond length was found in the range 2.16–2.42 Å.

3.2.4. *Transition state TS$_2$*

The calculated DFT optimized structures for the second transition states (TS_2) in the isomerization of **1–8** are summarized in Table 1 and are illustrated in Figure 2(d). Examination of the properties of the optimized geometries of the transition states revealed that all of them have similar structures. The breaking and forming bonds C–H and N–H were 1.54 Å and 1.30 Å, respectively. The bond angle N/H/C by which the base approaches the amine proton was 177°. The C–N bond length in all calculated TS2 was 1.47 Å and the C–C bond α to the carbonyl was in the range 1.53–1.54 Å.

3.2.5. *Intermediate INT$_2$*

The calculated B3LYP/6-31G(d,p) structures for the second tetrahedral intermediates in **1–8** (**1NT2-8INT2**) are illustrated in Figure 2(e) and their energies are depicted in Table 1. Inspection of the optimized structures of **1NT2-8INT2** revealed that the expected ion pair intermediate is not formed and instead there is a formation of a stable enol intermediate which is stabilized by a hydrogen bonding with an amine molecule (see INT2 in Scheme 2). It should be indicated that the energy difference between the ion pair and the enol form is relatively high and exceeds 10 kcal/mol in all eight systems studied. The relative stability of the enol form might be attributed to the fact that neutral molecules tend to be more stable than their corresponding ion pairs. Examination of the optimized structures of the intermediates demonstrated that all of them exhibit similar conformations by which the enol form is stabilized by two hydrogen bonds with the free amine molecule. One hydrogen bond is between the amine proton and the carbonyl oxygen and the other between the amine nitrogen and the enol proton. The first hydrogen bond in all calculated INT2 structures was found in the range 1.89–2.07 Å and that for the second hydrogen bond was 1.56–1.85 Å.

3.2.6. *Product (Trans isomers)*

DFT optimized geometries along with selected bond distances and bond angles for the *trans* isomers in **1–8** (**1*Trans*-8*Trans***) are illustrated in Figure 2(f), and are listed in Table 1. Careful inspection of the calculated geometries in Figure 2(f) indicates that all the geometries exhibit conformations by which the carboxyl group is engaged intermolecularly in a hydrogen bond with a free amine molecule via its nitrogen proton. The DFT calculated intermolecular hydrogen bonding length was found in the range 2.11 Å–2.21 Å. In addition, the calculated values for the C–C bond angles α to the carbonyl were in the range of 123.1°–123.6°. The C–C bond α to the carbonyl has similar value in all the trans structures with a length of 1.34 Å. It should be indicated that the optimized structures for all the trans isomers reside in a symmetrical orientation by which the two carbonyls are *anti* each to other.

3.3. *Mechanistic study of the amine-catalysed isomerization of 1–8*

3.3.1. *The rate-limiting step*

All entities involved in the proposed pathway illustrated in Scheme 2 were calculated using the DFT at B3LYP/6-31G (d,p) level of theory. The calculations were carried out in the gas phase (dielectric constant = 1), ether (dielectric constant = 4.5) and water (dielectric constant = 78.39). Using the calculated values for the enthalpy and entropy of the cis and the transition states in the isomerization of **1–8** (Table 1) the enthalpy activation energies ($\Delta H^{\ddagger}$), entropy activation energies ($T\Delta S^{\ddagger}$), and the free activation energies ($\Delta G^{\ddagger}$) for all steps (Scheme 2) were calculated and are summarized in Tables 2–4. A representation of the energy profiles for the isomerization processes **1–8** as calculated in the gas phase and water are shown in Figure 3. Careful examination of the data summarized in Tables 2–4 and graphically illustrated in Figure 3 demonstrated that the rate-limiting step for the amine-catalysed isomerization in **1–8** is a concerted step (step 1, barrier 1) by which an

Table 2. DFT (B3LYP) calculated kinetic and thermodynamic properties for the amine-catalysed isomerization of **1**–**8**.

System	log k_{exp}[6]	pk_a[35] Amine	Barrier 1 $\Delta H^{\ddagger}$	Barrier 1 $T\Delta S^{\ddagger}$	Barrier 1 $\Delta G^{\ddagger}$	Barrier 2 $\Delta H^{\ddagger}$	Barrier 2 $T\Delta S^{\ddagger}$	Barrier 2 $\Delta G^{\ddagger}$
1	−1.1878	10.73	12.83	−6.78	19.61	13.47	−3.2	16.67
2	−1.4157	10.64	10.73	−8.51	19.24	12.18	−6.56	18.74
3	−2.5045	10.63	11.59	−8.62	20.22	12.52	−6.55	19.07
4	−6.1979	4.63	24.11	−6.1	30.21	21.85	−5.7	27.55
5	−2.6271	9.34	15.65	−7.52	23.17	12.99	−3.28	16.27
6	−1.1158	11.22	15.24	1.34	13.90	13.1	6.09	7.01
7	–	9.5	14.84	−9.23	24.07	14.03	−5.67	19.7
8	–	10.71	11.50	−8.08	19.58	12.49	−6.4	18.89

Notes: B3LYP refers to values calculated by B3LYP/6-31G(d, p) method. $\Delta H^{\ddagger}$, $T\Delta S^{\ddagger}$ and $\Delta G^{\ddagger}$ are the calculated enthalpy, entropy and free activation energy (kcal/mol), respectively. Barrier 1 refers to the step by which INT1 is formed and barrier 2 refers to that in which INT2 is obtained (see Scheme 2). k_{exp} refers to the experimental isomerization rate.

Table 3. DFT (B3LYP) calculated kinetic and thermodynamic properties for the amine-catalysed isomerization of **1**–**8** as calculated in ether and water.

System	Barrier 1/ether $\Delta H^{\ddagger}$	Barrier 1/ether $\Delta G^{\ddagger}$	Barrier 2/ether $\Delta H^{\ddagger}$	Barrier 2/ether $\Delta G^{\ddagger}$	Barrier 1/water $\Delta H^{\ddagger}$	Barrier 1/water $\Delta G^{\ddagger}$	Barrier 2/water $\Delta H^{\ddagger}$	Barrier 2/water $\Delta G^{\ddagger}$
1	9.44	16.14	7.19	10.39	6.36	13.17	9.40	12.60
2	3.97	12.48	4.22	10.78	0	8.51	0.38	6.94
3	4.88	13.50	4.57	11.12	0.70	9.32	0.70	7.55
4	17.08	23.18	13.91	19.61	12.61	18.71	9.16	14.86
5	12.32	19.84	6.17	9.45	9.59	17.11	3.32	6.60
6	11.15	9.81	7.49	6.15	8.06	6.72	3.79	0
7	10.68	19.91	5.76	11.43	5.48	14.71	1.55	7.22
8	5.24	13.32	4.36	10.76	1.30	9.38	0.64	7.04

Notes: B3LYP refers to values calculated by B3LYP/6-31G(d, p) method. $\Delta H^{\ddagger}$, $T\Delta S^{\ddagger}$ and $\Delta G^{\ddagger}$ are the calculated enthalpy, entropy and free activation energy (kcal/mol), respectively. Barrier 1 refers to the step by which INT1 is formed and barrier 2 refers to that in which INT2 is obtained (see Scheme 2).

Table 4. DFT (B3LYP) calculated kinetic and thermodynamic properties for the amine-catalysed isomerization of **1**–**8** as calculated in the gas phase and water.

System	Gas Phase TS1	Gas Phase INT1	Gas Phase TS2	Gas Phase *Trans*	Water TS1	Water INT1	Water TS2	Water *Trans*
1	19.61	−8.39	16.67	−8.60	13.17	−12.72	12.6	−8.64
2	19.24	−8.32	18.74	−5.55	8.51	−18.31	6.94	−5.12
3	20.22	−8.43	19.07	−3.71	9.32	−18.48	7.55	−4.54
4	30.21	−8.30	27.55	−1.79	18.71	−17.84	14.86	−1.98
5	23.17	−9.53	16.27	−2.57	17.11	−19.16	6.60	0.85
6	13.90	−21.89	7.01	−16.90	6.72	−29.27	0	−18.46
7	24.07	−9.82	19.70	−6.87	14.71	−19.23	7.22	−6.62
8	19.58	−8.63	18.89	−6.31	9.38	−18.43	7.04	−5.90

Note: B3LYP refers to values calculated by B3LYP/6-31G(d, p) method.

amine molecule behaves as a nucleophile by approaching the C–C double bond and at the same time another amine molecule behaves as a base abstracting a proton from the tertiary amine adduct thus formed to give INT1 (see Scheme 2). On the other hand, the DFT calculation results for step 2 (barrier 2) in which an amine molecule behaves as a base by abstracting a proton from the β-carbon of INT1 indicate that the energy barrier for this process is lower than that in step 1. In addition, the calculation results indicate that the activation energy needed to give the trans isomer from INT2 is negligible. It is worth noting, that

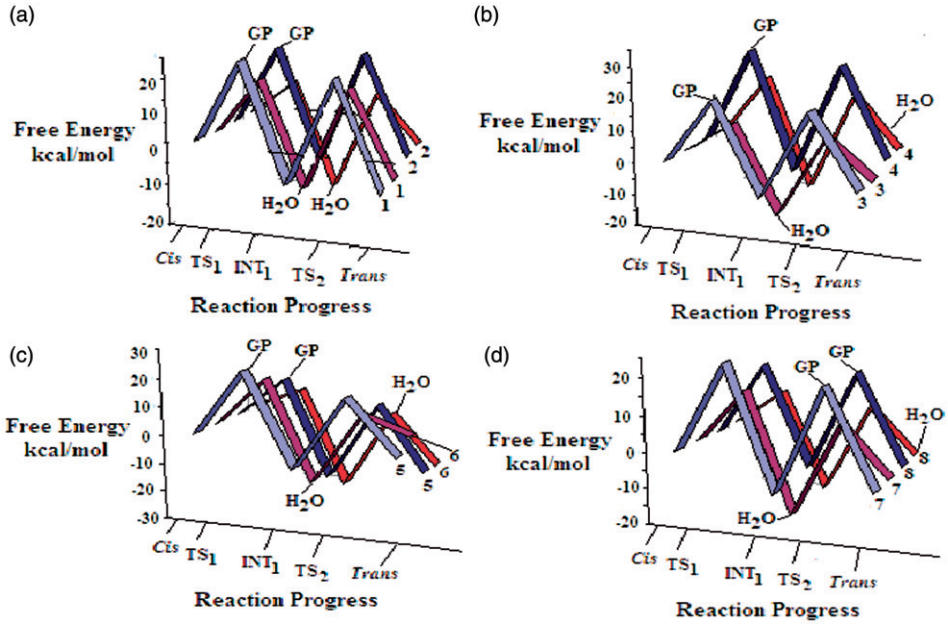

Figure 3. Representation of the isomerization energy profiles for systems **1**–**8**.

different paths other than that described in Scheme 2 were investigated, however, all other investigated pathways were found to have higher barriers than the one illustrated in Scheme 2.

3.3.2. *The factors affecting the isomerization rate*

3.3.2.1 *The nucleophilicity and basicity of the amine*. Inspection of the enthalpic energy values in Tables 2–3 indicates that the *cis-trans* isomerization is catalysed more efficiently by strong bases, because of their ability to readily donate a pair of electrons. For example the gas phase calculated activation energy for the isomerization catalysed by the strong base piperidine is 13.9 kcal/mol while that catalysed by the weak base aniline is 30.21 kcalmol. In fact when the gas phase enthalpic and free activation energies for step 1 (barrier 1, Scheme 2) were examined for correlation with the experimental rate good correlations were obtained with a correlation coefficient of $R = 0.93$ for the enthalpic energies and $R = 0.88$ for the free activation energies (Figure 4(a)). Furthermore, the DFT calculated energy data listed in Tables 2 and 3 was examined for correlation with the pK_a of the amine catalysts [35] used in processes **1**–**8**. The correlation results for the gas phase, ether and water calculated activation energies ($\Delta G^{\ddagger}$) for step 1 (barrier 1, Scheme 2) indicate good correlations with a correlation coefficient $R = 0.78$–0.90 (Figure 4(b)). Similarly, the enthalpic ($\Delta H^{\ddagger}$) and free activation energies ($\Delta G^{\ddagger}$) in step 2 (barrier 2, Scheme 2) were correlated with the experimental values. The correlation results indicate a moderate correlation between $\Delta G^{\ddagger}$ and log k_{exp} ($R^2 = 0.81$) whereas the correlation with the enthalpic energy values ($\Delta H^{\ddagger}$) was good, $R^2 = 0.92$ (Figure 4(c)). Figure 4(d) illustrates the correlation results of the gas phase, ether and water calculated enthalpic and free activation energies for step 2 (barrier 2, Scheme 2) with the basicity of the catalysts (pK_a of amine). The results demonstrate good correlations between the two parameters where the correlation coefficient R was in the range 0.76–0.97. In order to test whether the amine catalyst has the same effect on both barriers (barriers 1 and 2), the DFT calculated activation energies in the gas phase, ether and water for step 2 (barrier 2, $\Delta G^{\ddagger}$) were correlated with the activation energy values needed for step 1 (barrier 1, $\Delta G_B^{\dagger}$). The correlation results illustrated in Figure 5(a) indicate good correlations with a correlation coefficient $R = 0.89$, 0.73 and 0.74, respectively. This indicates that the driving force for the approach of the amine catalyst (nucleophilicity of the amine, step 1 in Scheme 2) and the proton abstraction by the amine (basicity of the amine, step 2 in Scheme 2) is the same. It should be indicated that the slopes of the three lines have different values; 1.06 for the energy values calculated in the gas phase, 0.61 for those calculated in the presence of ether and

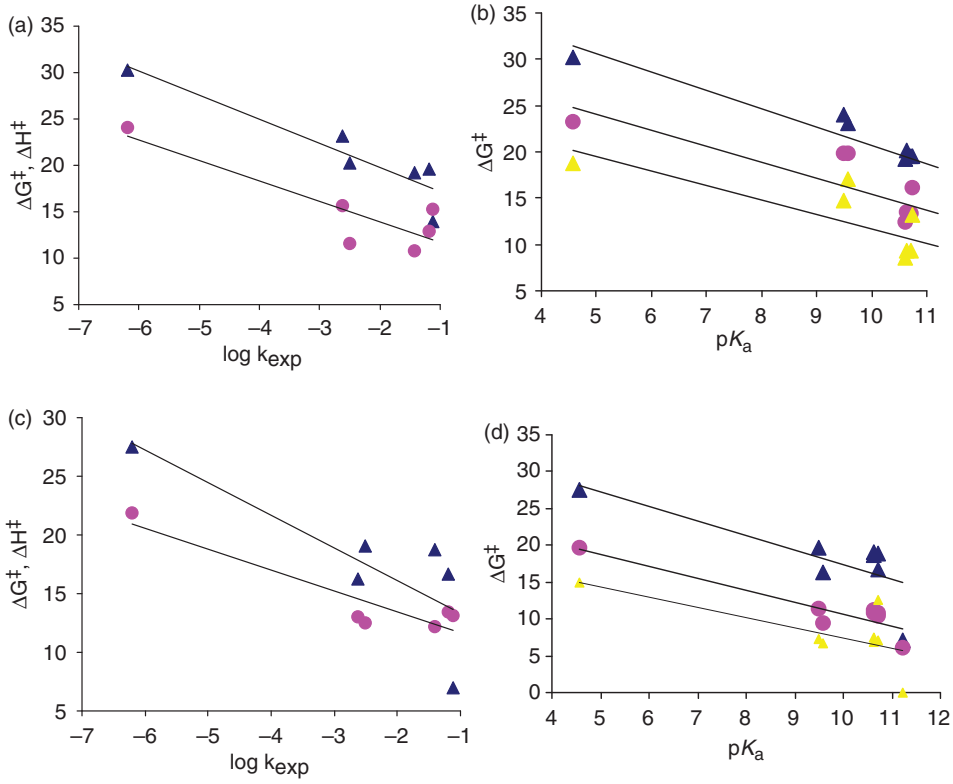

Figure 4. (a) Plot of the gas phase (GP) enthalpic, $\Delta H^{\ddagger}$ (circle points) and activation, $\Delta G^{\ddagger}$ (triangle points) energies for barrier 1 vs. the experimental isomerization rate (log k_{exp}) for processes **1**–**8**. (b) Plot of the activation energies ($\Delta G^{\ddagger}$) in the gas phase, GP (blue triangle points), ether (pink circle points) and H_2O (yellow triangle points) for barrier 1 vs. the basicity of the amine catalyst (pK_a) in systems **1**–**8**. (c) Plot of the gas phase (GP) enthalpic, $\Delta H^{\ddagger}$ (circle points) and activation, $\Delta G^{\ddagger}$ (triangle points) energies for barrier 2 vs. the experimental isomerization rate (log k_{exp}) for processes **1**–**8**. (d) Plot of the gas phase (GP) activation, $\Delta G^{\ddagger}$ (triangle points) and enthalpic, $\Delta H^{\ddagger}$ (circle points) energies for barrier 2 vs. the basicity of the amine catalyst (pK_a) in systems **1**–**8**. Barrier 1/GP refers to barrier 1 calculated in the gas phase. Barrier 1/GP/ether/H_2O refers to barrier 1 calculated in the gas phase, ether and water. Barrier 2/GP refers to barrier 2 calculated in the gas phase.

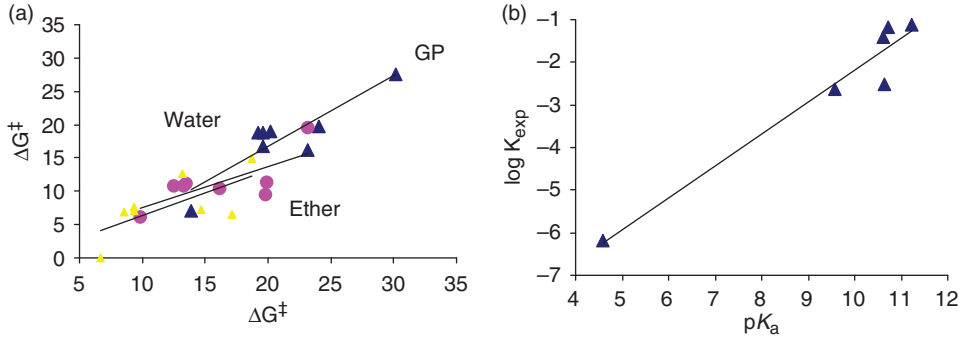

Figure 5. (a) Plot of the activation energy ($\Delta G^{\ddagger}$) for barrier 1 vs. the activation energy ($\Delta G^{\ddagger}$) for barrier 2 for processes **1–8** as calculated in the gas phase (blue triangle points), ether (pink circle points) and water (yellow triangle points). (b) Plot of the isomerization experimental rate (log k_{exp}) vs. the basicity of the amine catalyst (pK_a) in compounds **1–8**.

0.68 for those calculated in a dielectric constant 78.39 (water). The discrepancy in the slopes for the data in the gas phase and the data calculated in ether and water may be attributed to both factors nucleophilicity and basicity of the amine catalyst that are expected to be different according to the nature of the interactions between the solvent and the amine.

It should be emphasized that a distinction should be made between nucleophilicity and basicity. While step 1 in the isomerization is affected by both nucleophilicity and basicity of the amine catalyst, step 2 is

influenced solely by the ability of the amine to abstract a proton. Since step 1 is the rate-limiting step in the isomerization it is expected that both factors the basicity and the nucleophilicity of the amine will play dominant role in enhancing or inhibiting the reaction rate.

Furthermore, The experimental rate values listed in Table 2 were examined for correlation with the pK_a values of the amine catalysts [35] in processes **1**–**8**. The correlation results indicate excellent correlations between the two parameters with $R^2 = 0.97$ (Figure 5(b)). This indicates a linear relationship between the basic strength and the catalytic ability of the amine catalyst. However, this does not eliminate other factors affecting the isomerization rate.

3.3.2.2 *The effect of solvent on the isomerization rate*. The main objective of this study was to investigate the amine-catalysed isomerization of dimethyl maleate into dimethyl fumarate in order to utilize the former as a prodrug for the latter. Hence, it is necessary to investigate the mechanism of the reaction in water and other solvents in order to assess the effect of solvent (dielectric constant) on the reaction isomerization rate.

Careful examination of Tables 2–4 demonstrate that the activation and enthalpic energies for steps 1 and 2 (barriers 1 and 2) are largely affected by the nature of the solvent (dielectric constant). The calculated activation energies in the gas phase (dielectric constant = 1.0) were found to be higher than that calculated in ether (dielectric constant = 4.5) and the latter were higher than those calculated in water (dielectric constant = 78.39). The activation energy difference between the values calculated in the gas phase and water for step 1 (barrier 1) was in the range 6–11 kcal/mol and for step 2 (barrier 2) was 4–12 kcal/mol. A representation for such differences is illustrated graphically in Figure 3. The discrepancy might be attributed to the interaction between the solvent and the entities involved in the reaction pathway. While in the gas phase these interactions are negligible in water they are increased and as a result both transition states (TS1 and TS2) are much more stabilized which can result in reduced activation energy values.

4. Summary and conclusions

In summary, we conclude that the amine-catalysed isomerization of dialkyl maleate to dimethyl fumarate proceeds *via* four steps: (1) a concerted step by which a proton transfers from one amine molecule to another which subsequently enhances the addition of the adduct thus formed to the C–C double bond to yield INT1. (2) Abstraction of a proton from the β-carbon in INT1 by a second amine molecule to furnish intermediate, INT2. (3) Rotation about the C–C bond α to the carbonyl followed by proton abstraction by an amine molecule to yield unstable INT3, and (4) an elimination of an amine molecule to yield the trans isomer, dialkyl fumarate. Moreover, the DFT calculation results confirmed that the reaction is first order in dialkyl maleate, second order in the amine catalyst and overall third order. In addition, the calculations revealed an existence of linear correlation between the basicity (pK_a) of the amine catalyst and the isomerization rate. The reaction medium was found to have a significant effect on the isomerization rate. Polar solvents such as water tend to stabilize the transition states and consequently to facilitate the isomerization. The linear relationship between the DFT calculated data and the experimental data draw credibility for the use of DFT calculations to predict rates for other isomerization reactions. Furthermore, correlation of nucleophilicity and reactivity could be made via calculating the 'inherent nucleophilicity' from parameters such as polarizability, basicity and interaction energies in the transition states, which are independent of rate measurement**.** The reactivity series obtained in isomerization could be used to correlate attacks on other C–C double bonded systems, such as carbonyl carbon atoms.

Note

Supplementary material can be viewed online.

Supporting data

Calculation methods. Xyz Cartesian coordinates for the calculated optimized structures in processes **1**–**8**.

Acknowledgements

The Karaman Co. and the German-Palestinian-Israeli fund agency are thanked for support of our computational facilities. Special thanks are also given to Angi Karaman, Donia Karaman, Rowan Karaman and Nardene Karaman for technical assistance.

References

[1] K. Lohbeck, H. Haferkorn, W. Fuhrmann and N. Fedtke, Maleic and fumaric acids, in Ullmann's Encyclopedia of Industrial Chemistry (Wiley-VCH, Weinheim, 2000).

[2] M. Kodomari, T. Sakamoto and S. Yoshitomi, Bull. Chem. Soc. Jpn. **62**, 4053 (1989).
[3] M.M. Baag, A. Kar and N.P. Argade, Tetrahedron **59**, 6489 (2003).
[4] A.P. Doherty and K. Scott, J. Elctroanal. Chem. **30**, 35 (1998).
[5] G.R. Clemo and S.B. Graham, J. Chem. Soc. 213 (1930).
[6] K. Nozaki, J. Am. Chem. Soc. **63**, 2681 (1941).
[7] M. Davies and F.P. Evans, Trans. Faraday Soc. **51**, 1506 (1955).
[8] Z. Rappoport, C. Degani and S. Patai, J. Chem. Soc. 4513 (1963).
[9] A.G. Cook, A.B. Voges and A.E. Kammrath, Tetrahedron Lett. **42**, 7349 (2001).
[10] E. Janus, M. Lozynski and J. Pernak, Chem. Lett. **35**, 210 (2006).
[11] E.L. Eliel and S.H. Wilen, *Stereochemistry of Organic Compounds* (Wiley, New York, 1994), p. 580.
[12] S.W. Edwards and W.E. Knox, J. Biol. Chem. **220**, 79 (1956).
[13] S. Seltzer, J. Biol. Chem. **248**, 215 (1973).
[14] G. Polekhina, P.G. Board, A.C. Blackburn and M.W. Parker, Biochemistry **30**, 1567 (2001).
[15] U. Mrowietz, E. Christophers and P. Altmeyer, Br. J. Dermatol, **141**, 424 (1999).
[16] S. Schilling, S. Goelz, R. Linker, F. Luehder and R. Gold, Clin. Exp. Immunol. **145**, 101 (2006).
[17] L. Kappos, R. Gold, D.H. Miller, D.G. Macmanus, E. Havrdova,V. Limmroth, C.H. Polman, K. Schmierer, T.A. Yousry and M. Yang, for the BG-12 Phase IIb Study Investigators: *Lancet*, **372**, 1463 (2008).
[18] H. Wilms, J. Sievers, U. Rickert, M. Rostami-Yazdi, U. Mrowietz and R. Lucius, J. Neoroinflammation **7**, 30 (2010).
[19] R. Karaman and H. Hallak, Chem. Biol. Drug Design **76**, 350 (2010).
[20] R. Karaman, J. Comput. Mol. Des. **24**, 961 (2010).
[21] R. Karaman, Chem. Biol. Drug Design DOI: 10.1111/j.1747-0285.2011.01208.x (2011).
[22] H. Hejaz, R. Karaman and M. Khamis J. Mol. Modeling **18**, 103 (2012).
[23] R. Karaman, K.K. Dajani and H. Hallak, J. Mol. Modeling (DOI) 10.1007/s00894-011-1180-7 (2011).
[24] A.D. Becke, J. Chem. Phys. **98**, 5648 (1993).
[25] C. Lee, W. Yang and R.G. Parr, Phys. Rev. **37**, 785 (1988).
[26] P.J. Stevens, F.J. Devlin, C.F. Chablowski and M.J. Frisch, J. Phys. Chem. **98**, 11623 (1994).
[27] Gaussian 09, Revision A.1, M.J. Frisch, G.W. Trucks, H.B. Schlegel, G.E. Scuseria, M.A. Robb, J.R. Cheeseman, G. Scalmani, V. Barone, B. Mennucci, G.A. Petersson, H. Nakatsuji, M. Caricato, X. Li, H.P. Hratchian, A.F. Izmaylov, J. Bloino, G. Zheng, J.L. Sonnenberg, M. Hada, M. Ehara, K. Toyota, R. Fukuda, J. Hasegawa, M. Ishida, T. Nakajima, Y. Honda, O. Kitao, H. Nakai, T. Vreven, J.A. Montgomery, Jr., J.E. Peralta, F. Ogliaro, M. Bearpark, J.J. Heyd, E. Brothers, K.N. Kudin, V.N. Staroverov, R. Kobayashi, J. Normand, K. Raghavachari, A. Rendell, J.C. Burant, S.S. Iyengar, J. Tomasi, M. Cossi, N. Rega, J.M. Millam, M. Klene, J.E. Knox, J.B. Cross, V. Bakken, C. Adamo, J. Jaramillo, R. Gomperts, R. E. Stratmann, O. Yazyev, A.J. Austin, R. Cammi, C. Pomelli, J.W. Ochterski, R.L. Martin, K. Morokuma, V.G. Zakrzewski, G.A. Voth, P. Salvador, J.J. Dannenberg, S. Dapprich, A.D. Daniels, Ö. Farkas, J.B. Foresman, J.V. Ortiz, J. Cioslowski, and D.J. Fox, Gaussian, Inc., Wallingford CT, 2009.
[28] C.J. Casewit, K.S. Colwell and A.K. Rappe, J. Am. Chem. Soc. **114**, 10046 (1992).
[29] J.N. Murrell and K.J. Laidler, Trans Faraday Soc. **64**, 371 (1968).
[30] K. Muller, Angew Chem. Int. Ed. Engl. **19**, 1 (1980).
[31] M.T. Cancès, B. Mennucci and J. Tomasi, J. Chem. Phys. **107**, 3032 (1997).
[32] B. Mennucci and J. Tomasi, J. Chem. Phys. **106**, 5151 (1997).
[33] B. Mennucci, M.T. Cancès and J. Tomasi, J. Phys. Chem. B **101**, 10506 (1997).
[34] J. Tomasi, B. Mennucci and M.T. Cancès, J. Mol. Struct. (Theochem) **464**, 211 (1997).
[35] H.K. Hall Jr, J. Am. Chem. Soc. **79**, 5441 (1957).